

# Joint Transmitter–Receiver Optimization in Multitarget MIMO Radar

Kai Luo, *Member, IEEE*, and Athanassios Manikas, *Senior Member, IEEE*

**Abstract**—Although a significant attention has been drawn to the concept of multiple-input multiple-output (MIMO) radar and in particular on the transmit beamforming design and multitarget localization, the cooperation between the transmitter (Tx) and the receiver (Rx) has been rarely investigated. In this paper, a novel joint Tx and Rx optimization approach for localization is proposed for MIMO radar, where the transmit beamforming design and the estimation of the target’s complex path gain are jointly derived by solving an optimization problem that takes account various target parameters. Moreover, the proposed transmit beamforming design controls the power distribution per individual target. The performance of the proposed method is evaluated using computer simulation studies and compared with techniques which simply combine Tx beamforming design with multitarget localization methods.

**Index Terms**—MIMO radar, multitarget localization, beamforming.

## NOTATION

$a, A$	Scalar.
$\underline{a}, \underline{A}$	Vector.
$\mathbb{A}$	Matrix.
$\underline{0}_N$	$N \times 1$ vector of zeros.
$\mathbb{I}_N$	$N \times N$ identity matrix.
$(\cdot)^T, (\cdot)^H$	Transpose and Hermitian transpose.
$(\cdot)^*$	Complex conjugate.
$\lceil \cdot \rceil$	Round up to integer.
$ \cdot $	Absolute value.
$\ \cdot\ $	Euclidean norm.
$\ \cdot\ _F$	Frobenius norm.
$\mathcal{E}\{\cdot\}$	Expectation operator.
$\text{Tr}\{\cdot\}$	Trace.
$\text{Re}\{\cdot\}$	Real part of a complex number.
$\exp(\underline{a})$	Elementwise exponential of vector $\underline{a}$ .
$\mathcal{C}$	Field of complex numbers.
$\mathbb{P}_{\mathbb{A}}^\perp$	Complement projection matrix of subspace spanned by the columns of $\mathbb{A}$ .

Manuscript received October 12, 2016; revised April 14, 2017 and June 4, 2017; accepted June 28, 2017. Date of publication July 13, 2017; date of current version September 30, 2017. The associate editor coordinating the review of this manuscript and approving it for publication was Dr. Paolo Braca. The work of K. Luo was supported by the National Natural Science Foundation of China under Grant 61501193. (*Corresponding author: Athanassios Manikas.*)

K. Luo was with Imperial College London, London SW7 2AZ, U.K. He is now with the School of Electronics Information and Communications, Huazhong University of Science and Technology, Wuhan 430073, China (e-mail: kluo@hust.edu.cn).

A. Manikas is with the Department of Electrical and Electronic Engineering, Imperial College London, London SW7 2AZ, U.K. (e-mail: a.manikas@imperial.ac.uk).

Color versions of one or more of the figures in this paper are available online at <http://ieeexplore.ieee.org>.

Digital Object Identifier 10.1109/TSP.2017.2726993

## I. INTRODUCTION

A MULTIPLE-INPUT MULTIPLE-OUTPUT (MIMO) radar [1]–[3] is a system which employs multiple antennas at both the transmitter (Tx) and receiver (Rx) emitting orthogonal waveforms through the Tx array and processing echoes received by the Rx array. According to the array configuration, MIMO radars can be mainly classified into two types. One type employs large aperture arrays [2] at both Tx and Rx. This kind of MIMO radar systems deals with an extended target model which contains rich scatterers. The large aperture arrays at both Tx and Rx enable MIMO radar to view different aspects of a target from different angles simultaneously. In other words, the large aperture arrays exploits the spatial diversity of the target’s radar cross section (RCS) to reduce the scintillation effects. Rather than distributing Tx and Rx antennas in a large area, the other type employs small aperture arrays for both the Tx and Rx sites so that MIMO radar views the same aspect of a target from the same angle (monostatic radar [3], [4]) or different angles for Tx and Rx arrays (bistatic radar [3]). In this case, point targets in the far field of MIMO radar are assumed. With the transmit waveform diversity, MIMO radar with small aperture arrays at both Tx and Rx achieves flexible transmit beampattern design [5], [6] and enhances the ability of multitarget localization [7]. This paper is concerned with small aperture arrayed monostatic MIMO radar.

Recent work in small aperture arrayed MIMO radar mainly focuses on the multitarget localization [8]–[15] and the transmit beamforming design [5], [6], [16], [17]. The parameters including DOA, Doppler and range of targets are normally assumed unknown in the multitarget–localization scenario. Thus, the orthogonal waveforms are usually utilized in the MIMO radar in order to provide an equivalent gain for the whole space and keep the echoes from the multiple targets uncorrelated to each other within a single pulse period. Thus, many direction finding algorithms employed in passive and active radars can be applied directly for the multitarget localization in MIMO radar such as Least Squares (LS), Capon, Amplitude and Phase Estimation (APES) [8], [9], ESPRIT [10], [11] and Iterative Adaptive Approach (IAA) [12] [18], etc. In [14] a multitarget localization method for MIMO radar with mutual target interference cancellation capabilities has been proposed, outperforming the existing methods. However, the advantages offered by transmitting orthogonal waveforms are based on the sacrifice of high directional gain obtained by the transmit beamforming design. Having limited power and transmitting orthogonal waveforms leads to the degradation of the resolution and accuracy of tar-

gets' locations. On the other hand, due to the flexibility in the choice of the transmitted waveforms in the MIMO radar, some work related to transmit beamforming has been done. For instance, in [5], [6] the aim is to design the covariance matrix of the probing waveforms in order to approach a desired transmit beampattern. Furthermore, in [16], [17] the transmit beamforming is in a form called transmit subaperturing approach or transmit array partitioning. Thus, with transmit beamforming, a radar system can provide high directional gain which can enhance the performance of the multitarget localization, especially the resolution capabilities and the estimation accuracy of various target parameters of interest.

Therefore, an intuitive way to let the multitarget localization of MIMO Radar enjoy the benefits provided by the transmit beamforming is the joint Tx–Rx optimization based on a multitarget localization strategy. This may work in an iterative way where the estimates of targets' locations by the Rx array are based on the Tx beams which are generated corresponding to the previous estimates of the targets' locations. However, most recent designs of the transmit beams aim to match a desired beampattern such as an approximately rectangular beampattern [5], [6]. Moreover, for the desired beampattern, the values of the directional gains for the pre-known targets are preset without any criteria. In fact, with limited transmit power, it is difficult to set these values directly due to the lack of the knowledge of the targets' locations. Therefore, the current beampattern matching designs are not suitable for the joint Tx–Rx multitarget localization. In [5], a method named maximum power design is proposed for the transmit beamforming. In this beamforming method, the beams are formed using the eigenvector associated with the maximum eigenvalue of the covariance matrix composed by the manifold vectors of known directions of targets. Thus, this maximum power method can be simply employed by the joint Tx–Rx multitarget localization. However, this design maximizes the total power at the directions of targets of interest while the distributed power for individual target is not controlled. Hence, this joint Tx–Rx multitarget localization may fail to work due to the lack of energy illuminated on some of the targets.

Inspired by the joint Tx–Rx beamforming for MIMO communications [19]–[21], a novel joint Tx–Rx optimization approach for multitarget localization is proposed in this paper. In the proposed approach, the transmit beamforming matrix is generated by solving an optimization problem which takes account of not only the previous estimates of the directions but also the estimates of delays and path gains of targets. Moreover, a novel multitarget DOA and delay estimation method based on the current transmit beamforming matrix is presented. It is worth noting that the proposed approach allows the control of the Tx power illuminated at each target's location by solving a constrained optimization problem. Thus, the proposed joint Tx–Rx multitarget localization approach achieves higher resolution and more accurate estimation of targets' locations than the methods which simply combine the transmit beamforming in multitarget localization.

The main contribution of this paper is to propose a novel MIMO radar system with enhanced resolution capabilities and

target parameter estimation accuracy. This takes into account not only the geometries of both Tx and Rx antenna arrays but also the relative target path delays and directions. It uses the concept of the array manifold of both Tx–array and Rx–array which are functions of targets directions. Furthermore, it is based on solving a joint transmitter–receiver optimization problem, using the data collected over a small observation interval of  $L$  snapshots and under various constraints/conditions for each target. In the proposed approach, the following target parameters are estimates:

- directions,
- delays (relative to the receiver's reference clock/point),
- complex path gains (reflection coefficients),

in conjunction with:

- the weight vector of the Rx–beamformer, and
- the weight matrix of a multibeam Tx beamformer.

In particular, an iterative approach is presented which takes into account the inter-dependence of the Tx, Rx and target parameters. This provides (during the observation interval of  $L$  snapshots) an iterative estimation of several multi-target parameters plus the weight matrix of the multibeam Tx beamformer which is then “copied” into the transmitter.

The rest of this paper is organized as follows. Section II describes the MIMO radar system model. In Section III, an MSE–based optimization problem for the joint Tx–Rx multitarget localization is proposed and its solutions are derived. Based on this optimization problem, a multitarget DOA and delay estimation method is proposed. Utilizing the results of Section III, a novel joint Tx–Rx multitarget localization approach is presented in Section IV. Although clutter-suppression is not the main aim of this paper, a simple and efficient way of handling the clutter effects is presented in Section V. In particular, the clutter-plus-noise can be seen as “color-noise” and this section presents an approach for “whitening” the clutter-plus-noise effects. Following this, computer simulation results are presented in Section VI and finally the paper is concluded in Section VII.

## II. SIGNAL MODEL

Consider a narrowband MIMO radar system with the Tx array of  $N_{Tx}$  antennas and the Rx array of  $N_{Rx}$  antennas. It is assumed that both the Tx and Rx arrays are calibrated with known geometries and common reference point (“colocated”, monostatic radar). Thus, each target is at the same location with respect to both Tx and Rx arrays. Without loss of generality, the Tx array, the Rx array and the targets are located in a two-dimensional space with the targets at the far–field of the radar.

At the Tx array,  $N_{Tx}$  pulsed waveforms  $m_i(t)$ ,  $i = 1, 2, \dots, N_{Tx}$  which have good auto- and cross-correlation properties are utilized. That is, if  $\underline{m}(t)$  is defined as

$$\underline{m}(t) = [m_1(t), m_2(t), \dots, m_{N_{Tx}}(t)]^T, \quad (1)$$

then

$$\mathcal{E}\{m_i(t)m_j(t-\tau)\} = \begin{cases} 1, & i = j, \tau = 0 \\ 0 & \text{otherwise} \end{cases} \quad (2)$$

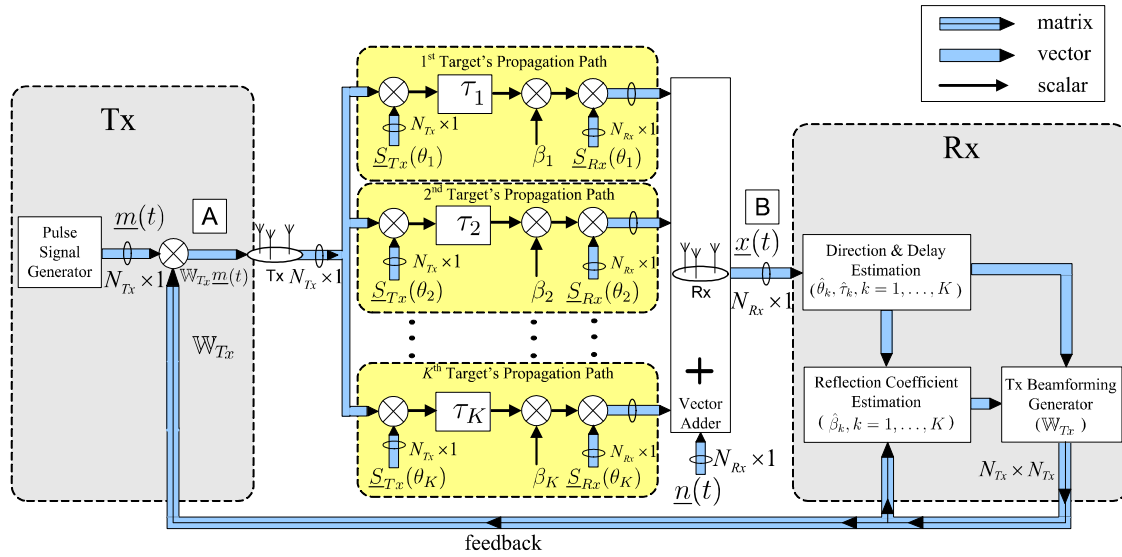


Fig. 1. The equivalent baseband MIMO radar system based on the proposed joint Tx and Rx multitarget localization method.

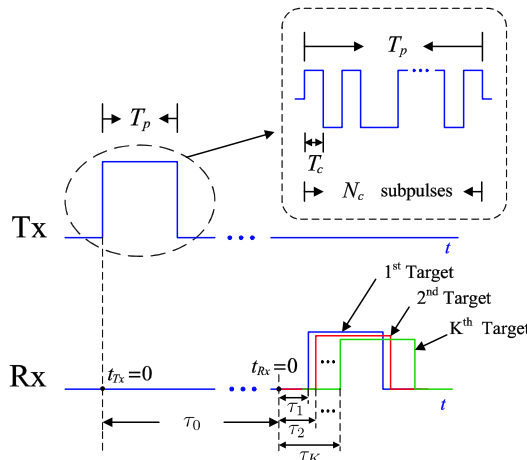


Fig. 2. The configuration of baseband transmitted pulses and the echoes impinging on the Rx array from different targets in MIMO radar system.

$\forall i, j = 1, \dots, N_{T_x}$ .<sup>1</sup> These waveforms are linearly combined for each antenna of Tx array according to the Tx beamforming matrix  $\mathbb{W}_{T_x} \in \mathbb{C}^{N_{T_x} \times N_{T_x}}$ , i.e. a multi-beam beamformer (see Point-A in Fig. 1).

Assuming there are  $K$  point targets at distinct directions<sup>2</sup>  $\theta_k, k = 1, 2, \dots, K$  with respect to the radar's common reference point (i.e. the origin of the Cartesian coordinate system). Then, the transmitted waveforms are reflected by multiple targets and received by the Rx array. Fig. 2 shows the configuration and the propagation of pulses along the time axis. Thus, ignoring the common delay  $\tau_0$  for simplicity (i.e. the time reference

<sup>1</sup>Note that (2) reflects the ideal correlation properties of the waveforms  $\underline{m}(t)$  which, in practice, can be achieved using Hadamard sequences or gold-sequences which are generated by modulo-two addition of m-sequences.

<sup>2</sup>Without any loss of generality, the elevation angle is assumed equal to zero, i.e. all targets are located on the  $(x, y)$  plane.

is taken at the receiver,  $t_{R_x} = 0$ ), the equivalent baseband received vector-signal  $\underline{x}(t)$  (see Point-B in Fig. 1) can be written as

$$\begin{aligned} \underline{x}(t) &\triangleq [x_1(t), x_2(t), \dots, x_{N_{R_x}}(t)]^T \\ &= \sum_{k=1}^K \beta_k \underline{S}_{R_x}(\theta_k) \underline{S}_{T_x}^H(\theta_k) \mathbb{W}_{T_x} \underline{m}(t - \tau_k) + \underline{n}(t) \end{aligned} \quad (3)$$

where  $\underline{S}_{T_x}(\theta_k) \in \mathbb{C}^{N_{T_x} \times 1}$  and  $\underline{S}_{R_x}(\theta_k) \in \mathbb{C}^{N_{R_x} \times 1}$  denote the manifold vectors of the Tx and Rx arrays respectively for the  $k^{th}$  target, which are defined as

$$\underline{S}_{R_x}(\theta_k) \triangleq \exp(-j [\underline{r}_x, \underline{r}_y, \underline{r}_z]_{R_x} \underline{k}(\theta_k)) \quad (4)$$

$$\underline{S}_{T_x}(\theta_k) \triangleq \exp(j [\underline{r}_x, \underline{r}_y, \underline{r}_z]_{T_x} \underline{k}(\theta_k)) \quad (5)$$

with  $\theta_k$  denoting the azimuth angle. In (4) and (5), the matrices  $[\underline{r}_x, \underline{r}_y, \underline{r}_z]_{R_x}$  and  $[\underline{r}_x, \underline{r}_y, \underline{r}_z]_{T_x}$  denote the Cartesian coordinates of the Rx and Tx antenna-array elements, respectively, and

$$\underline{k}(\theta_k) = \frac{2\pi F_c}{c} [\cos \theta_k, \sin \theta_k]^T \quad (6)$$

is the wavenumber vector (pointing towards the target at the direction  $\theta_k$ ) with  $F_c$  denoting the carrier frequency and  $c$  representing the velocity of light. Furthermore, in (3), the matrix  $\mathbb{W}_{T_x}$  is the transmit beamforming matrix, the parameter  $\beta_k$  denotes the reflection coefficient associated with the  $k^{th}$  target and  $\underline{n}(t)$  is the isotropic complex Gaussian noise vector [22] of  $\mathbb{Q}_{N_{R_x}}$  mean and covariance  $\sigma_n^2 \mathbb{I}_{N_{R_x}}$ , i.e.  $\mathcal{N}(\underline{0}_{N_{R_x}}, \sigma_n^2 \mathbb{I}_{N_{R_x}})$ .

With reference to Fig. 2, each transmit waveform has pulsewidth  $T_p$  and consists of  $N_c$  subpulses, each of duration  $T_c = T_p/N_c$ . Thus, the delay of the  $k^{th}$  target is quantized as follows:

$$\ell_k = \lceil \tau_k / T_c \rceil \bmod N_c, k = 1, \dots, K. \quad (7)$$

Note that the period of a subpulse  $T_c$  is the minimum recognized delay which is proportional to the range resolution (the size of range bin) [23].

Then the discretized received data matrix  $\mathbb{X} \in \mathcal{C}^{N_{Rx} \times L}$  can be given according to (3):

$$\mathbb{X} = \sum_{k=1}^K \beta_k \underline{\mathcal{S}}_{Rx}(\theta_k) \underline{\mathcal{S}}_{Tx}^H(\theta_k) \mathbb{W}_{Tx} \mathbb{M} \mathbb{J}^{\ell_k} + \mathbb{N} \quad (8)$$

where  $L = N_c + Q$  is the number of snapshots (subpulses), in which  $Q$  refers to the maximum tolerable delay. Furthermore, the matrix  $\mathbb{M} \in \mathcal{C}^{N_{Tx} \times L}$  denotes the zero-appended transmitted waveform matrix and  $\mathbb{J}$  represents the  $(L \times L)$  time upper shift matrix which is defined as

$$\mathbb{J} = \begin{bmatrix} \mathbf{0}_{L-1}, & \mathbb{I}_{L-1} \\ 0, & \mathbf{0}_{L-1}^T \end{bmatrix}. \quad (9)$$

In such a MIMO radar system,  $\theta_k$ ,  $\beta_k$  and  $\ell_k$  are the unknown parameters to be estimated for the localization of the  $k^{th}$  target, where

- $\theta_k$  describes the direction of the target,
- the complex path gain  $\beta_k$  incorporates the effects of the reflection material of target and its magnitude is inversely proportional to the power of the distance of the target [24], and
- the delay  $\ell_k$  indicates the relative distance of the  $k^{th}$  target from the Rx reference clock (i.e.  $t_{Rx} = 0$ ).

### III. FRAMEWORK OF JOINT TX AND RX MSE-BASED OPTIMIZATION

For the aim of improving the multitarget localization at Rx by iteratively updating the Tx beamforming matrix according to the estimates given by the previous targets' localizations, a joint Tx-Rx multitarget localization approach (as illustrated in Fig. 1) is proposed. Firstly, inspired by the APES method [9], the design of Tx beamforming matrix and the estimation of target's path gain are derived from the following constrained optimization problem:

$$\min_{\beta_k, \mathbb{W}_{Tx}, \underline{\mathcal{W}}_{Rx,k}} \|\underline{\mathcal{W}}_{Rx,k}^H \mathbb{X} - \beta_k \underline{\mathcal{S}}_{Tx}^H(\theta_k) \mathbb{W}_{Tx} \mathbb{M} \mathbb{J}^{\ell_k}\|^2 \quad (10a)$$

$$\text{subject to } \underline{\mathcal{S}}_{Rx}^H(\theta_k) \underline{\mathcal{W}}_{Rx,k} = 1, \forall k \quad (10b)$$

where  $\underline{\mathcal{W}}_{Rx,k}$  is the Rx beamforming vector for the  $k^{th}$  target. The output of this Rx beamformer should be as close as possible to a signal which only includes the parameters for the  $k^{th}$  target (i.e.,  $\beta_k \underline{\mathcal{S}}_{Tx}^H(\theta_k) \mathbb{W}_{Tx} \mathbb{M} \mathbb{J}^{\ell_k}$ ). An alternative framework is described next where initially the vectors  $\underline{\mathcal{W}}_{Rx,k}$  and  $\beta_k$  are expressed in terms of the matrix  $\mathbb{W}_{Tx}$ . Then an iterative approach is formulated (see Section IV) to reach the solution to the optimization problem of (10).

#### A. The Optimal Rx Beamforming Vector $\underline{\mathcal{W}}_{Rx}$

For the  $k^{th}$  target, with fixed  $\beta_k$  and  $\mathbb{W}_{Tx}$ , (10) becomes a constrained minimization problem with respect to  $\underline{\mathcal{W}}_{Rx,k}$ .

That is

$$\min_{\underline{\mathcal{W}}_{Rx,k}} \|\underline{\mathcal{W}}_{Rx,k}^H \mathbb{X} - \beta_k \underline{\mathcal{S}}_{Tx}^H(\theta_k) \mathbb{W}_{Tx} \mathbb{M} \mathbb{J}^{\ell_k}\|^2 \quad (11a)$$

$$\text{subject to } \underline{\mathcal{S}}_{Rx}^H(\theta_k) \underline{\mathcal{W}}_{Rx,k} = 1 \quad (11b)$$

which can be solved by using the Lagrange multiplier methodology. If  $\xi_k$  denotes the unconstrained augmented objective function of (11), then

$$\begin{aligned} \xi_k = & \underline{\mathcal{W}}_{Rx,k}^H \mathbb{R}_{xx} \underline{\mathcal{W}}_{Rx,k} + |\beta_k|^2 \underline{\mathcal{S}}_{Tx}^H(\theta_k) \mathbb{W}_{Tx} \mathbb{R}_{xm}^{(k)} \mathbb{W}_{Tx}^H \underline{\mathcal{S}}_{Tx}(\theta_k) \\ & - \beta_k \underline{\mathcal{S}}_{Tx}^H(\theta_k) \mathbb{W}_{Tx} (\mathbb{R}_{xm}^{(k)})^H \underline{\mathcal{W}}_{Rx,k} \\ & - \beta_k^* \underline{\mathcal{W}}_{Rx,k}^H \mathbb{R}_{xm}^{(k)} \mathbb{W}_{Tx}^H \underline{\mathcal{S}}_{Tx}(\theta_k) \\ & + \text{Re} \{ \lambda (\underline{\mathcal{W}}_{Rx,k}^H \underline{\mathcal{S}}_{Rx}(\theta_k) - 1) \} \end{aligned} \quad (12)$$

where

$$\mathbb{R}_{xx} = \frac{1}{L} \mathbb{X} \mathbb{X}^H, \quad (13)$$

$$\mathbb{R}_{xm}^{(k)} = \frac{1}{L} \mathbb{X} (\mathbb{M} \mathbb{J}^{\ell_k})^H, \quad (14)$$

$$\mathbb{R}_{mm}^{(k)} = \frac{1}{L} \mathbb{M} \mathbb{J}^{\ell_k} (\mathbb{M} \mathbb{J}^{\ell_k})^H. \quad (15)$$

Setting the derivative of the cost function  $\xi_k$  with respect to  $\underline{\mathcal{W}}_{Rx,k}$  to zero, i.e.

$$\frac{\partial \xi_k}{\partial \underline{\mathcal{W}}_{Rx,k}} = \mathbf{0}_{N_{Rx}} \quad (16)$$

provides

$$\underline{\mathcal{W}}_{Rx,k} = \beta_k^* \mathbb{R}_{xx}^{-1} \mathbb{R}_{xm}^{(k)} \mathbb{W}_{Tx}^H \underline{\mathcal{S}}_{Tx}(\theta_k) - \frac{1}{2} \lambda \mathbb{R}_{xx}^{-1} \underline{\mathcal{S}}_{Rx}(\theta_k). \quad (17)$$

Then, substituting (17) into the constraint of the minimization problem in (11b) yields the solution for the Lagrange multiplier  $\lambda$

$$\lambda = \frac{2 \left( \beta_k^* \underline{\mathcal{S}}_{Rx}^H(\theta_k) \mathbb{R}_{xx}^{-1} \mathbb{R}_{xm}^{(k)} \mathbb{W}_{Tx}^H \underline{\mathcal{S}}_{Tx}(\theta_k) - 1 \right)}{\underline{\mathcal{S}}_{Rx}^H(\theta_k) \mathbb{R}_{xx}^{-1} \underline{\mathcal{S}}_{Rx}(\theta_k)}. \quad (18)$$

Finally, inserting (18) back into (17) and rearranging gives the solution for  $\underline{\mathcal{W}}_{Rx,k}$

$$\begin{aligned} \underline{\mathcal{W}}_{Rx,k} = & \beta_k^* \left( \mathbb{I}_{N_{Rx}} - \frac{\mathbb{R}_{xx}^{-1} \underline{\mathcal{S}}_{Rx}(\theta_k) \underline{\mathcal{S}}_{Rx}^H(\theta_k)}{\underline{\mathcal{S}}_{Rx}^H(\theta_k) \mathbb{R}_{xx}^{-1} \underline{\mathcal{S}}_{Rx}(\theta_k)} \right) \\ & \times \mathbb{R}_{xx}^{-1} \mathbb{R}_{xm}^{(k)} \mathbb{W}_{Tx}^H \underline{\mathcal{S}}_{Tx}(\theta_k) \\ & + \frac{\mathbb{R}_{xx}^{-1} \underline{\mathcal{S}}_{Rx}(\theta_k)}{\underline{\mathcal{S}}_{Rx}^H(\theta_k) \mathbb{R}_{xx}^{-1} \underline{\mathcal{S}}_{Rx}(\theta_k)}, \forall k = 1, \dots, K. \end{aligned} \quad (19)$$

It is worth to point out that these Rx beamforming vectors  $\underline{\mathcal{W}}_{Rx,k} \forall k = 1, \dots, K$  are the essential intermediate solutions used for the derivation of the solutions  $\beta_k \forall k = 1, \dots, K$  and  $\mathbb{W}_{Tx}$  and will be used in the proposed approach in the next section.

#### B. The Estimation of Complex Path Gain $\beta$

The estimation of complex path gain is obtained from the solution  $\beta_k$  to the optimization problem in (10) for a given



$\mathbb{W}_{Tx}$ . Firstly, considering the optimization problem in (10) with the fixed  $\mathbb{W}_{Tx}$  and  $\underline{w}_{Rx,k}$  for the  $k^{th}$  target. That is,

$$\min_{\beta_k} \|\underline{w}_{Rx,k}^H \mathbb{X} - \beta_k \underline{S}_{Tx}^H(\theta_k) \mathbb{W}_{Tx} \mathbb{M} \mathbb{J}^{\ell_k}\|^2. \quad (20)$$

Let the derivative of the object function in (20) with respect to the complex path gain  $\beta_k$  equal zero, i.e.

$$\begin{aligned} & \left( \beta_k^* \underline{S}_{Tx}^H(\theta_k) \mathbb{W}_{Tx} \mathbb{R}_{mm}^{(k)} \mathbb{W}_{Tx}^H \underline{S}_{Tx}(\theta_k) \right)^T \\ & - \left( \underline{S}_{Tx}^H(\theta_k) \mathbb{W}_{Tx} (\mathbb{R}_{xm}^{(k)})^H \underline{w}_{Rx,k} \right)^T = 0. \end{aligned} \quad (21)$$

Then after rearranging, the solution of the complex path gain  $\beta_k$  can be expressed as

$$\beta_k = \frac{\underline{w}_{Rx,k}^H \mathbb{R}_{xm}^{(k)} \mathbb{W}_{Tx}^H \underline{S}_{Tx}(\theta_k)}{\underline{S}_{Tx}^H(\theta_k) \mathbb{W}_{Tx} \mathbb{R}_{mm}^{(k)} \mathbb{W}_{Tx}^H \underline{S}_{Tx}(\theta_k)}. \quad (22)$$

Thus, substituting  $\underline{w}_{Rx,k}^H$  given by (19) into (22) yields (23), shown at the bottom of this page, which provides the estimation of the complex path gain  $\beta_k$ . It is now clear from (23) that the complex path gain  $\beta_k$  of target is a function of only three parameters. These are the Tx beamforming matrix  $\mathbb{W}_{Tx}$ , the  $k^{th}$  target's DOA  $\theta_k$  and the delay  $\ell_k$ . This implies that the complex path gain  $\beta_k$  of the  $k^{th}$  target can be estimated if Tx beamforming matrix  $\mathbb{W}_{Tx}$ , DOAs  $\theta_k$  and delays  $\ell_k$  are known. However, these parameters remain unknown and we will focus next on designing  $\mathbb{W}_{Tx}$  and estimating  $\theta_k$  and  $\ell_k$  for every target, i.e.  $\forall k$ .

### C. Designing the Tx Beamforming Matrix $\mathbb{W}_{Tx}$

Intuitively, the solution of  $\mathbb{W}_{Tx}$  should be given by solving the minimization problem in (10) with fixed  $\beta_k$  and  $\underline{w}_{Rx,k} \forall k = 1, \dots, K$ . That is, the minimization problem of (10) is modified as follows

$$\min_{\mathbb{W}_{Tx,k}} \|\underline{w}_{Rx,k}^H \mathbb{X} - \beta_k \underline{S}_{Tx}^H(\theta_k) \mathbb{W}_{Tx,k} \mathbb{M} \mathbb{J}^{\ell_k}\|^2, \forall k = 1, \dots, K \quad (24)$$

where the solution  $\mathbb{W}_{Tx,k}$  can be obtained by setting the derivative of the cost function in (24) equal to  $\mathbb{O}_{N_{Tx} \times N_{Tx}}$ , which gives the expression

$$|\beta_k|^2 \underline{S}_{Tx}(\theta_k) \underline{S}_{Tx}^H(\theta_k) \mathbb{W}_{Tx,k} \mathbb{R}_{mm}^{(k)} = \beta_k^* \underline{S}_{Tx}(\theta_k) \underline{w}_{Rx,k}^H \mathbb{R}_{xm}^{(k)}. \quad (25)$$

Then, inserting (19) into (25) yields

$$\begin{aligned} & \beta_k \underline{S}_{Tx}^H(\theta_k) \mathbb{W}_{Tx,k} \mathbb{A}_k = \underline{B}_k^T \\ \Rightarrow & \underline{S}_{Tx}^H(\theta_k) \mathbb{W}_{Tx,k} = \frac{1}{\beta_k} \underline{B}_k^T \mathbb{A}_k^{-1} \end{aligned} \quad (26)$$

where

$$\begin{aligned} \mathbb{A}_k &= \mathbb{R}_{mm}^{(k)} - (\mathbb{R}_{xm}^{(k)})^H \mathbb{R}_{xx}^{-1} \mathbb{R}_{xm}^{(k)} \\ &+ \frac{(\mathbb{R}_{xm}^{(k)})^H \mathbb{R}_{xx}^{-1} \underline{S}_{Rx}(\theta_k) \underline{S}_{Rx}^H(\theta_k) \mathbb{R}_{xx}^{-1} \mathbb{R}_{xm}^{(k)}}{\underline{S}_{Rx}^H(\theta_k) \mathbb{R}_{xx}^{-1} \underline{S}_{Rx}(\theta_k)}, \end{aligned} \quad (27)$$

$$\underline{B}_k = \left( \frac{\underline{S}_{Rx}^H(\theta_k) \mathbb{R}_{xx}^{-1} \mathbb{R}_{xm}^{(k)}}{\underline{S}_{Rx}^H(\theta_k) \mathbb{R}_{xx}^{-1} \underline{S}_{Rx}(\theta_k)} \right)^T. \quad (28)$$

Note that (26) represents a set of equations with more unknown than the number of equations. Taking into account that  $\underline{S}_{Tx}^H(\theta_k) \underline{S}_{Tx}(\theta_k) = N_{Tx}$ , an analytical solution of the matrix  $\mathbb{W}_{Tx,k}$  for the  $k^{th}$  target that satisfies (26) is given as follows

$$\mathbb{W}_{Tx,k} = \frac{1}{\beta_k N_{Tx}} \underline{S}_{Tx}(\theta_k) \underline{B}_k^T \mathbb{A}_k^{-1} \quad (29)$$

and this is valid for every target, i.e.  $\forall k$ .

Finally, for the purpose of forming beams towards the locations of all the  $K$  targets, the Tx beamforming matrix  $\mathbb{W}_{Tx}$  is generated by the summation of the normalized beamforming matrix  $\mathbb{W}_{Tx,k}$ ,  $k = 1, \dots, K$ , i.e.

$$\mathbb{W}_{Tx} = \sum_{k=1}^K \frac{\mathbb{W}_{Tx,k}}{\|\mathbb{W}_{Tx,k}\|_F}, \quad (30)$$

Eqn. (30) can be deployed in a MIMO radar systems subject that the DOAs, delays and complex path gains (as shown in Fig. 1) of the targets can be estimated and this is our next task. It is important to note that the Tx beamforming matrix  $\mathbb{W}_{Tx}$  has to be normalized according to the constraint of the maximum transmit power in radar systems.

### D. Proposed Multitarget DOA and Delay Estimation Method

In the previous discussion, the estimation of the complex path gain  $\beta_k$  and the design of Tx beamforming  $\mathbb{W}_{Tx}$  were presented, based on the assumption that the locations of multiple targets, i.e., the DOAs  $\theta_k$  and delays  $\ell_k$ ,  $\forall k = 1, \dots, K$  of the  $k^{th}$  target are pre-known or pre-estimated. Therefore, the estimation of these two critical sets of parameters ( $\theta_k$ ,  $\ell_k$ ),  $\forall k = 1, \dots, K$  are needed. Here, a joint DOA and delay estimation method based on a spatial-temporal spectrum search is proposed which is defined as follows

$$\xi(\theta, \ell) = \frac{\underline{w}_{Rx}^H(\theta, \ell) \mathbb{R}_{xx} \underline{w}_{Rx}(\theta, \ell)}{\|\underline{w}_{Rx}^H(\theta, \ell) \mathbb{X} - \beta(\theta, \ell) \underline{S}_{Tx}^H(\theta) \mathbb{W}_{Tx} \mathbb{M} \mathbb{J}^{\ell}\|^2} \quad (31)$$

where the vector  $\underline{w}_{Rx}(\theta, \ell)$  is given by (34) (derived from (19)) and  $\beta(\theta, \ell)$  is the optimal solution of (23) for the complex path

$$\beta_k = \frac{\underline{S}_{Rx}^H(\theta_k) \mathbb{R}_{xx}^{-1} \mathbb{R}_{xm}^{(k)} \mathbb{W}_{Tx}^H \underline{S}_{Tx}(\theta_k)}{\underline{S}_{Rx}^H(\theta_k) \mathbb{R}_{xx}^{-1} \underline{S}_{Rx}(\theta_k) \underline{S}_{Tx}^H(\theta_k) \mathbb{W}_{Tx} \left( \mathbb{R}_{mm}^{(k)} - (\mathbb{R}_{xm}^{(k)})^H \mathbb{R}_{xx}^{-1} \mathbb{R}_{xm}^{(k)} \right) \mathbb{W}_{Tx}^H \underline{S}_{Tx}(\theta_k) + \|\underline{S}_{Rx}^H(\theta_k) \mathbb{R}_{xx}^{-1} \mathbb{R}_{xm}^{(k)} \mathbb{W}_{Tx}^H \underline{S}_{Tx}(\theta_k)\|^2} \quad (23)$$

gain, re-expressed in the form of (35) where  $\mathbb{R}_{xm}^\ell$  and  $\mathbb{R}_{mm}^\ell$  are defined as

$$\mathbb{R}_{xm}^\ell = \frac{1}{L} \mathbb{X}(\mathbb{M}\mathbb{J}^\ell)^H, \quad (32)$$

$$\mathbb{R}_{mm}^\ell = \frac{1}{L} \mathbb{M}\mathbb{J}^\ell (\mathbb{M}\mathbb{J}^\ell)^H. \quad (33)$$

and (34) and (35), shown at the bottom of this page.

Note that in (31), the denominator is the proposed MSE criterion in (10) while the numerator is the power of the beamformer's output signal power and the overall cost function is used to find the  $(\theta, \ell)$  that maximizes this ratio, i.e. simultaneously maximizes the numerator and minimizes the denominator. Thus, in (31), a two-dimensional search is needed for finding the peaks whose coordinates are referring to the estimates of all targets' DOAs and delays, respectively. Moreover, it is important to point out that in this paper it is assumed that the number of targets is known. This number (detection problem) can be estimated using existing criteria, such as AIC [25], MDL [26], Gershgorin disks [27], etc.

#### IV. JOINT TX AND RX MULTITARGET LOCALIZATION APPROACH

##### A. Proposed Joint Tx and Rx Multitarget Localization

From the above analysis, it can be seen that, with estimated DOAs and delays of targets, the Tx beamforming matrix and the estimates of the complex path gains are functions of each other. Thus a joint method is proposed for the multitarget localization in MIMO Radar via several iterative steps.

For the  $i^{th}$  iteration and based on the Tx beamforming matrix  $\mathbb{W}_{Tx}^{[i-1]}$  from the previous iteration, the DOAs  $\theta_k^{[i]}$  and the delays  $\ell_k^{[i]}, k = 1, \dots, K$  of targets are estimated by the multitarget localization methods in Section III-D.

Then, the estimates of the complex path gains  $\beta_k^{[i]}, k = 1, \dots, K$  are obtained by (23).

Finally, based on these estimated parameters  $\theta_k^{[i]}, \ell_k^{[i]}, \beta_k^{[i]}, k = 1, \dots, K$ , the Tx beamforming matrix  $\mathbb{W}_{Tx}^{[i]}$  is updated according to (30).

The initial Tx beamformer should evenly distribute the transmit power towards all the directions due to no prior knowledge of the locations of targets. Thus, an identity matrix is utilized, i.e.  $\mathbb{W}_{Tx} = \mathbb{I}_{N_{Tx}}$ . A summary of the proposed joint multitarget localization approach is given in Table I.

TABLE I  
PROPOSED JOINT TX AND RX MULTITARGET LOCALIZATION

<b>initialize</b>
1 For $[i] = 0$ , set the Tx beamformer matrix $\mathbb{W}_{Tx}^{[0]} = \mathbb{I}_{N_{Tx}}$
2 Set the index $[i] = 1$
<b>repeat</b>
3 Calculate $\mathbb{R}_{xx}, \mathbb{R}_{xm}^{(k)}$ and $\mathbb{R}_{mm}^{(k)}$ using Eqns. (13)–(15)
4 Estimate $\hat{\theta}_k^{[i]}$ and $\hat{\ell}_k^{[i]}, k = 1, \dots, K$ using Eqn. (31) provided in Sec. III-D
5 Evaluate $\hat{\beta}_k^{[i]}, k = 1, \dots, K$ according to Eqn. (35) with $\mathbb{W}_{Tx}^{[i-1]}$ and estimated $\hat{\theta}_k^{[i]}, \hat{\ell}_k^{[i]}, k = 1, \dots, K$
6 Evaluate the Tx beamforming matrix $\mathbb{W}_{Tx}^{[i]}$ based on estimated $\hat{\theta}_k^{[i]}, \hat{\ell}_k^{[i]}, \hat{\beta}_k^{[i]}, k = 1, \dots, K$ according to Eqns. (29) and (30)
7 Update the index $[i] \rightarrow [i + 1]$
<b>until</b> a predefined convergence criterion is reached

##### B. Proposed Approach Using two Alternative Tx-Beamformers

In the Step-6 of the proposed approach, which is given in Table I, we have used a novel Tx weight matrix which is given by (29) and (30). Here, two other Tx beamformers are introduced which can be utilized in Step-6 instead of (29) and (30).

The first Tx beamformer is the maximum power design which is concerned with maximizing the total power at the estimated directions  $(\hat{\theta}_k, k = 1, \dots, K)$  of targets [5] and is based on the following constrained optimization problem

$$\max_{\mathbb{W}_{Tx}} \text{Tr} \left\{ \underline{S}_{Tx}^H(\hat{\theta}) \mathbb{W}_{Tx} \underline{S}_{Tx}(\hat{\theta}) \right\} \quad (36a)$$

$$\text{subject to } \text{Tr} \left\{ \mathbb{W}_{Tx}^H \mathbb{W}_{Tx} \right\} = 1 \quad (36b)$$

where

$$\underline{S}_{Tx}(\hat{\theta}) = \left[ \underline{S}_{Tx}(\hat{\theta}_1), \underline{S}_{Tx}(\hat{\theta}_2), \dots, \underline{S}_{Tx}(\hat{\theta}_K) \right] \quad (37)$$

Then, the optimum solution is obtained as follows

$$\mathbb{W}_{Tx} = \left[ \underline{E}_{\max}, \mathbb{O}_{N_{Tx} \times (N_{Tx} - 1)} \right] \quad (38)$$

in which  $\underline{E}_{\max}$  is the eigenvector corresponding to the largest eigenvalue of the matrix  $\underline{S}_{Tx}(\hat{\theta}) \underline{S}_{Tx}^H(\hat{\theta})$ .

The second Tx beamformer is the weighted manifold vectors (WMV) of the estimated targets' directions [22]. The WMV method forms the Tx beams via weighting the manifold vectors of the estimated directions of the targets with their estimated

$$\underline{w}_{Rx}(\theta, \ell) = \beta^*(\theta, \ell) \left( \mathbb{I}_{N_{Rx}} - \frac{\underline{S}_{Rx}^{-1}(\theta) \underline{S}_{Rx}^H(\theta)}{\underline{S}_{Rx}^H(\theta) \underline{S}_{Rx}^{-1}(\theta)} \right) \mathbb{R}_{xx}^{-1} \mathbb{R}_{xm}^\ell \mathbb{W}_{Tx}^H \underline{S}_{Tx}(\theta) + \frac{\mathbb{R}_{xx}^{-1} \underline{S}_{Rx}(\theta)}{\underline{S}_{Rx}^H(\theta) \mathbb{R}_{xx}^{-1} \underline{S}_{Rx}(\theta)} \quad (34)$$

$$\beta(\theta, \ell) = \frac{\underline{S}_{Rx}^H(\theta) \mathbb{R}_{xx}^{-1} \mathbb{R}_{xm}^\ell \mathbb{W}_{Tx}^H \underline{S}_{Tx}(\theta)}{\underline{S}_{Rx}^H(\theta) \mathbb{R}_{xx}^{-1} \underline{S}_{Rx}(\theta) \underline{S}_{Tx}^H(\theta) \mathbb{W}_{Tx} \left( \mathbb{R}_{mm}^{(k)} - (\mathbb{R}_{xm}^\ell)^H \mathbb{R}_{xx}^{-1} \mathbb{R}_{xm}^\ell \right) \mathbb{W}_{Tx}^H \underline{S}_{Tx}(\theta) + \left\| \underline{S}_{Rx}^H(\theta) \mathbb{R}_{xx}^{-1} \mathbb{R}_{xm}^\ell \mathbb{W}_{Tx}^H \underline{S}_{Tx}(\theta) \right\|^2} \quad (35)$$

path gains, as follows

$$\mathbb{W}_{Tx} \triangleq [\mathbb{S}_{Tx}(\hat{\theta}), \mathbb{O}_{N_{Tx} \times (N_{Tx} - K)}] \text{diag} \left\{ \hat{\underline{\beta}}^* \right\} \quad (39)$$

where

$$\hat{\underline{\beta}} = \left[ \hat{\beta}_1, \hat{\beta}_2, \dots, \hat{\beta}_K, 0, \dots, 0 \right]^T \quad (40)$$

It is worth noting that the Tx beamforming matrix needs to be normalized to keep the same total transmit power.

In the next section, the proposed novel beamformer given by (29)/(30) will be examined by computer simulation studies. Furthermore, for comparison, the two Tx beamformers, given by (38) and (39), will be also examined as part of the Step-6 of our proposed multitarget DOA and delay estimation approach.

## V. CLUTTER EFFECTS

In the previous sections the radar operates in the presence of targets and additive spatially white Gaussian noise. That is, “clutter-free” case is assumed. In the presence of clutter the signal model of (3) becomes

$$\begin{aligned} \underline{x}(t) = & \underbrace{\sum_{k=1}^K \beta_k \underline{S}(\theta_k) \underline{S}_{Tx}^H(\theta_k) \mathbb{W}_{Tx} \underline{m}(t - \tau_k)}_{\triangleq \underline{x}_c(t)} \\ & + \underline{x}_c(t) + \underline{n}(t). \end{aligned} \quad (41)$$

where  $\underline{x}_c(t)$  denotes the received signal vector associated with the clutter. In (41) the sum of clutter and noise terms is not spatially white anymore but it belongs to the family of spatially color-noise. Therefore, it is intuitive to mitigate the clutter in a similar way as the color-noise whitening process used in antenna array signal processing [22]. In this case the second order statistics (covariance matrix) of  $\underline{x}(t)$  can be expressed as follows:

$$\begin{aligned} \mathbb{R}_{xx} = & \mathcal{E} \left\{ \underline{x}(t) \underline{x}^H(t) \right\} \\ = & \underbrace{\mathcal{E} \left\{ \underline{x}_t(t) \underline{x}_t^H(t) \right\}}_{\triangleq \mathbb{R}_t} + 2 \text{Re} \underbrace{\mathcal{E} \left\{ \underline{x}_t(t) \underline{x}_c^H(t) \right\}}_{\triangleq \mathbb{R}_{tc}} \\ & + \underbrace{\mathcal{E} \left\{ \underline{x}_c(t) \underline{x}_c^H(t) \right\} + \mathcal{E} \left\{ \underline{n}(t) \underline{n}^H(t) \right\}}_{\triangleq \mathbb{R}_{c+n}}, \end{aligned} \quad (42)$$

Due to the good correlation properties of transmit signals, it is assumed that the clutter and the targets are located in different range bins<sup>3</sup>, which implies that  $\mathbb{R}_{tc} \simeq \mathbb{O}_{N_{Rx}}$ , i.e. the covariance matrix between the echo from target and clutter can be ignored.

In (42), the matrix  $\mathbb{R}_{c+n}$  denotes the covariance matrix of the clutter plus noise, which can be decomposed, using eigendecomposition, as follows

$$\mathbb{R}_{c+n} = \mathbb{E} \mathbb{D} \mathbb{E}^H, \quad (43)$$

where  $\mathbb{E} \in C^{N_{Rx} \times N_{Rx}}$  is a unitary matrix with columns the eigenvectors of  $\mathbb{R}_{c+n}$  and  $\mathbb{D}$  is a diagonal matrix where its  $k^{th}$

<sup>3</sup>Note that the range bin is defined by the interval  $T_c$  (see Fig. 2), which is very small. Any two paths with delays greater than  $T_c$  have correlation  $\simeq 0$

TABLE II  
REDEFINING PARAMETERS TO HANDLE CLUTTER

clutter free	redefined parameters (clutter)
$\underline{x}(t)$	$\underline{x}(t) \triangleq \mathbb{T} \underline{x}(t)$
$\mathbb{X}$	$\mathbb{X} \triangleq \mathbb{T} \mathbb{X}$
$\mathbb{R}_{xx}$	$\mathbb{R}_{xx} \triangleq \mathbb{T} \mathbb{R}_{xx} \mathbb{T}^H$
$\mathbb{R}_{xm}$	$\mathbb{R}_{xm} \triangleq \mathbb{T} \mathbb{R}_{xm}$
$\underline{S}_{Rx}$	$\underline{S}_{Rx} \triangleq \mathbb{T} \underline{S}_{Rx}$

diagonal element  $d_k$  is the eigenvalue corresponding to the  $k^{th}$  eigenvector in  $\mathbb{E}$ . That is,

$$\mathbb{D} = \text{diag} \{ d_1, d_2, \dots, d_{N_{Rx}} \} \quad (44)$$

Based on the above, let us define a transformation matrix  $\mathbb{T}$  as follows

$$\mathbb{T} \triangleq \mathbb{D}^{-\frac{1}{2}} \mathbb{E}^H \in C^{N_{Rx} \times N_{Rx}}, \quad (45)$$

By applying  $\mathbb{T}$  to the received signal  $\underline{x}(t)$ , the clutter term can be “isotropically whitened”, which implies the covariance matrix of clutter-plus-noise  $\mathbb{R}_{c,n}$  is effectively transformed into an identity matrix. Indeed,

$$\begin{aligned} \mathbb{T} \mathbb{R}_{xx} \mathbb{T}^H &= \mathbb{T} (\mathbb{R}_t + \mathbb{R}_{c+n}) \mathbb{T}^H \\ &= \mathbb{T} \mathbb{R}_t \mathbb{T}^H + \underbrace{\mathbb{D}^{-\frac{1}{2}} \mathbb{E}^H \mathbb{R}_{c+n} \mathbb{E} \mathbb{D}^{-\frac{1}{2}}}_{= \mathbb{I}_{N_{Rx}} \text{ (using (43))}} \end{aligned} \quad (46)$$

Therefore, by applying the preprocess matrix  $\mathbb{T}$  at the received data, the target-plus-clutter case can be transformed to an equivalent clutter-free case where  $\mathbb{T}$  can be estimated by the data collected in the absence of the targets. To transform the equations of Sections III and IV to the target-plus-clutter case, some parameters should be redefined as shown in Table II.

It is also worth noting that if the clutter is not present in the radar’s environment, the transformation  $\mathbb{T}$  is simplified to an identity matrix.

## VI. COMPUTER SIMULATION RESULTS

In this section, the performance of the proposed joint Tx–Rx multitarget localization approach is validated using computer simulation studies of 2000 Monte Carlo trials. Consider a set of  $N_{Tx}$  gold sequences of length  $N_c = 127$  are generated for the transmit waveforms of a MIMO radar system and assume the maximum tolerable delay to be  $Q = 25$ . Without loss of generality, the total transmit power  $P_T$  is set to 1. The root-mean-square errors (RMSEs) of the estimated parameters  $\hat{\theta}_k, \hat{\ell}_k, \hat{\beta}_k, k = 1, \dots, K$  are utilized to evaluate the performances of the proposed approach and are defined as follows

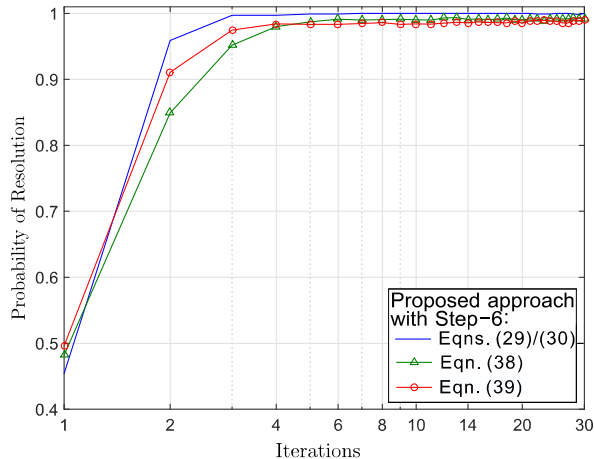
$$\text{RMSE}_{\theta} = \frac{1}{K} \sum_{k=1}^K \sqrt{\mathcal{E} \left\{ |\hat{\theta}_k - \theta_k|^2 \right\}} \quad (47)$$

$$\text{RMSE}_{\tau} = \frac{1}{K} \sum_{k=1}^K \sqrt{\mathcal{E} \left\{ |\hat{\ell}_k - \ell_k|^2 \right\}} \quad (48)$$

$$\text{RMSE}_{\beta} = \frac{1}{K} \sum_{k=1}^K \sqrt{\mathcal{E} \left\{ |\hat{\beta}_k - \beta_k|^2 \right\}} \quad (49)$$

TABLE III  
 PROPOSED JOINT TX AND RX MULTITARGET LOCALIZATION

Target	1 <sup>st</sup>	2 <sup>nd</sup>	3 <sup>rd</sup>
DOA $\theta$	60°	106°	112°
Path gain $\beta$	0.9exp(j1.1)	0.7exp(j0.7)	0.6exp(j1.9)
Delay $\ell$	0	15	20


 Fig. 3. The resolution probability versus iterations for the proposed approach. The Tx and Rx arrays are UCAs with ( $N_{Tx} = 10, N_{Rx} = 15$ ) and half-wavelength interelement spacing.

Furthermore, the probability of resolution, which is defined as the number of trials that all the targets can be successfully resolved [28] divided by the total number of trials for each iteration, is also employed as a performance criterion.

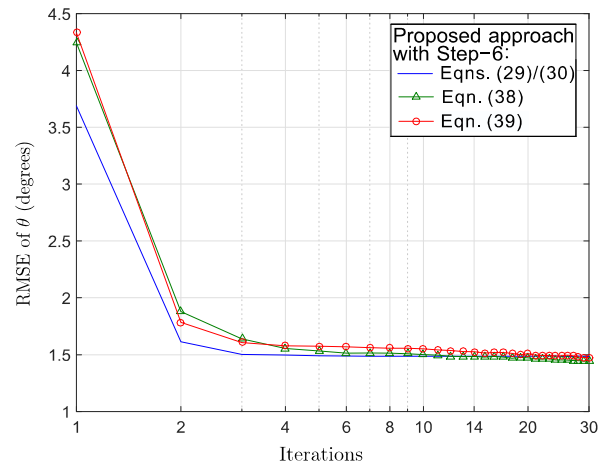
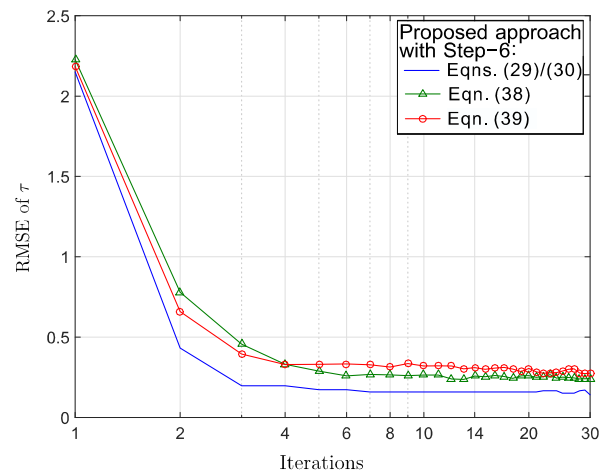
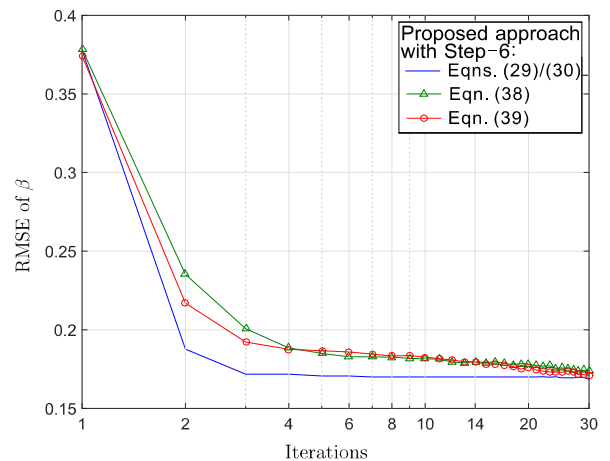
In all simulations, it is assumed that there are  $K = 3$  targets located as shown in Table III. The received signal is corrupted by an isotropic complex Gaussian noise of zero mean and covariance  $\sigma_n^2 \mathbb{I}_{N_{Rx}}$  with  $\sigma_n^2 = 100$ , i.e.,  $P_T/\sigma_n^2 = -20$  dB. In each simulation, the proposed iterative localization algorithm will use three different Tx beamforming designs (for comparison) given by (29) and (30), (38) and (39).

#### Case 1:

Consider a MIMO radar system in which two uniform circular arrays (UCAs) with  $N_{Tx} = 10, N_{Rx} = 15$  antennas are deployed in Tx and Rx, respectively, with half-wavelength interelement spacing.

Since there is no prior knowledge about the targets, the transmit power is uniformly distributed in space at the first iteration. Thereafter, the transmit power focuses on the estimated locations of the targets. Thus, the resolution probability of all the methods increases steeply for the few iterations as shown in Fig. 3. Better than Tx-weights given by (38) and (39), the resolution probability of the proposed Tx-weight vector given by (29) and (30) reaches 1 after several iterations. Moreover, the proposed Tx-weight converges faster than the other two, which implies less pulses are needed for the target localization.

Moreover, the RMSEs of the estimated targets' parameters ( $\hat{\theta}_k, \hat{\ell}_k, \hat{\beta}_k, k = 1, \dots, K$ ) are given in Figs. 4–6, respectively. Figs. 4 and 6 show that, after the 20th iteration, (38) and


 Fig. 4. The  $RMSE_\theta$  convergence for the proposed approach. The Tx and Rx arrays are UCAs with ( $N_{Tx} = 10, N_{Rx} = 15$ ) and half-wavelength interelement spacing.

 Fig. 5. The  $RMSE_\tau$  convergence of the proposed approach. The Tx and Rx arrays are UCAs with ( $N_{Tx} = 10, N_{Rx} = 15$ ) and half-wavelength interelement spacing.

 Fig. 6. The  $RMSE_\beta$  convergence of the proposed approach. The Tx and Rx arrays are UCAs with ( $N_{Tx} = 10, N_{Rx} = 15$ ) and half-wavelength interelement spacing.



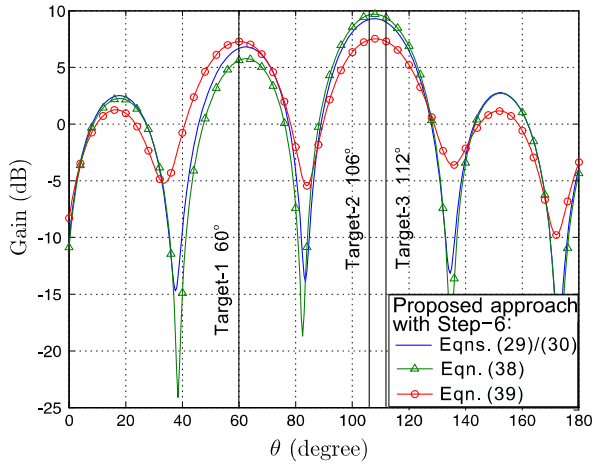


Fig. 7. The Tx beampatterns for the proposed approach at the 20<sup>th</sup> iteration when Tx and Rx arrays are UCAs with ( $N_{Tx} = 10, N_{Rx} = 15$ ) and half-wavelength interelement spacing.

(39) achieve slightly better estimation of the targets' DOA and complex path gains than (29)/(30). This is due to the power allocation tradeoff between the direction towards the target at  $\theta_1 = 60^\circ$  and the direction towards the two closely spacing targets at ( $\theta_2 = 106^\circ, \theta_3 = 112^\circ$ ). Indeed, Fig. 7 shows that, at the 20th iteration, (39) provides higher gain towards the target at  $\theta_1 = 60^\circ$  and (38) provides higher gain towards ( $\theta_2 = 106^\circ, \theta_3 = 112^\circ$ ) than the Tx-weight matrix of (29)/(30) (note that in Fig. 7 the solid vertical lines represent the true values of the targets' directions). However, (39) almost provides equal gain towards these two directions while apparently more energy has to be allocated to the direction towards the two closely spaced targets at ( $\theta_2 = 106^\circ, \theta_3 = 112^\circ$ ) in order to be able to resolve them. Besides, (38) is unable to control the power distribution for individual target since it only aims to maximize the total power illuminated on all the target without any power constraint for the individual targets. Thus, the resulting powers at the directions of targets might be rather different from one another due to different array geometries and directions of targets. Consequently, some targets may not be detected if insufficient power illuminates these targets. Nevertheless, (29)/(30) controls the power at the direction of each target to avoid this problem.

Furthermore, (29)/(30) provides better estimation of the targets' delays than the other two Tx-weights as shown in Fig. 5 since it takes account of the estimates of targets' delays in the design of Tx beamforming. It is worth to note that (29)/(30) achieves a faster convergence than the other weights, which implies less pulses are needed for the multitarget localization. Figure 8 shows the spectrum of the proposed multitarget DOA and delay estimation approach.

#### Case 2:

Consider the same scenario as Case 1 but with ( $N_{Tx} = 10, N_{Rx} = 15$ ) uniform linear Tx and Rx arrays (ULAs) of half-wavelength interelement spacing. In this case, (38) fails to work while (29)/(30) provides better performance than (39).

Fig. 9 shows the Tx beampatterns of (29)/(30) as well as (39) at the 20<sup>th</sup> iteration as well as (38) at the iteration just

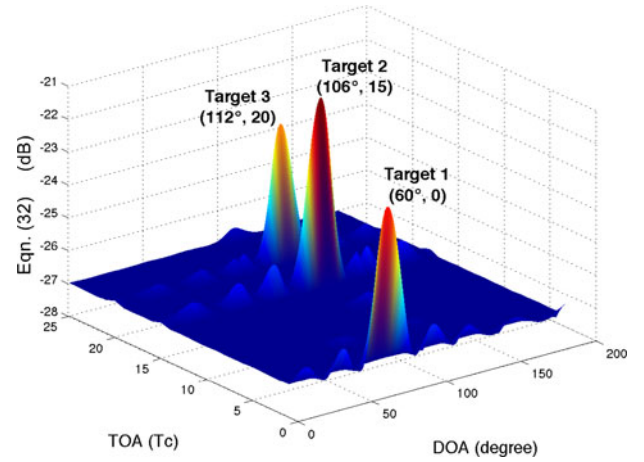


Fig. 8. The spectrum of the proposed multitarget DOA and delay estimation at the 20<sup>th</sup> iteration according to (31). The Tx and Rx arrays are UCAs with ( $N_{Tx} = 10, N_{Rx} = 15$ ) and half-wavelength interelement spacing.

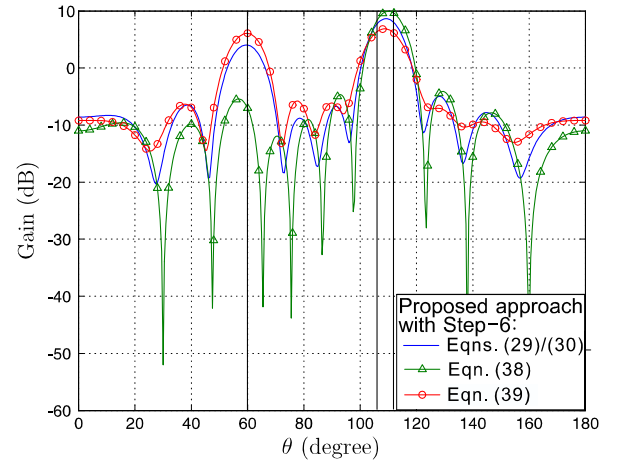


Fig. 9. The Tx beam patterns for the proposed approach at the 20<sup>th</sup> iteration for (29)/(30) and (39). The Tx and Rx arrays are ULAs with ( $N_{Tx} = 10, N_{Rx} = 15$ ) and half-wavelength interelement spacing. The Tx beam pattern for (38) is also shown at the iteration just before it fails.

before it fails. As seen from this figure, by the maximum power method, the transmit power is mainly allocated towards the targets at  $\theta_2 = 106^\circ, \theta_3 = 112^\circ$  (around 10 dB) while the target at  $\theta_1 = 60^\circ$  is illuminated by less power (less than -5 dB) since the geometry of the Tx and Rx array is changed from UCAs to ULAs. Consequently, the target at  $\theta_1 = 60^\circ$  is not resolved by (38). Moreover, Fig. 10 shows the resolution probability of the proposed Tx weight vector given by (29)/(30). For comparison, in Fig. 10 the resolution probability of (39), LS and Capon methods are also shown. Furthermore, Figs. 11–13 depict the RMSEs of the estimated targets' parameters ( $\hat{\theta}_k, \hat{\ell}_k, \hat{\beta}_k, k = 1, \dots, K$ ). As shown in all these figures, (29)/(30) significantly outperforms (39) in both the resolution probability and multitarget parameter estimation error<sup>4</sup>. Besides, the proposed joint Tx–Rx approach either with (29)/(30)

<sup>4</sup>It is important to point out that in the presence of clutter, using the transformation  $\mathbb{T}$ , we get similar results.

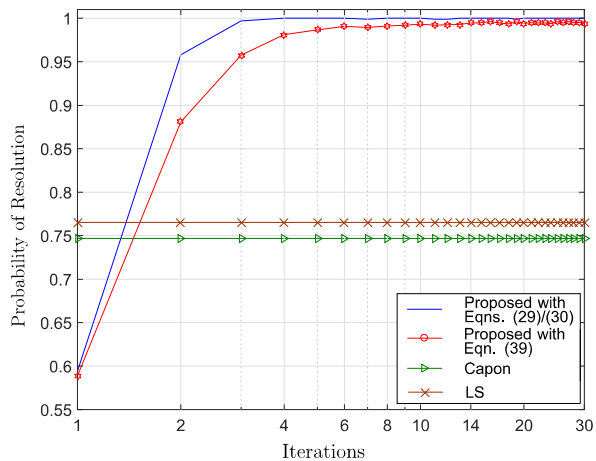


Fig. 10. The resolution probability of the proposed approach. The Tx and Rx arrays are ULAs with ( $N_{Tx} = 10, N_{Rx} = 15$ ) and half-wavelength interelement spacing.

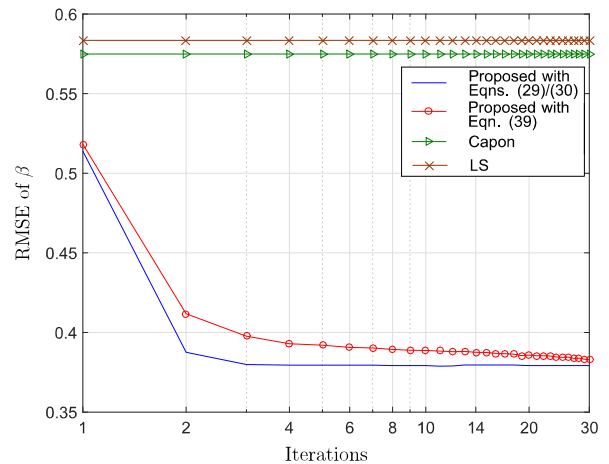


Fig. 13. The  $RMSE_{\beta}$  convergence of the proposed approach. The Tx and Rx arrays are ULAs with ( $N_{Tx} = 10, N_{Rx} = 15$ ) and half-wavelength interelement spacing.

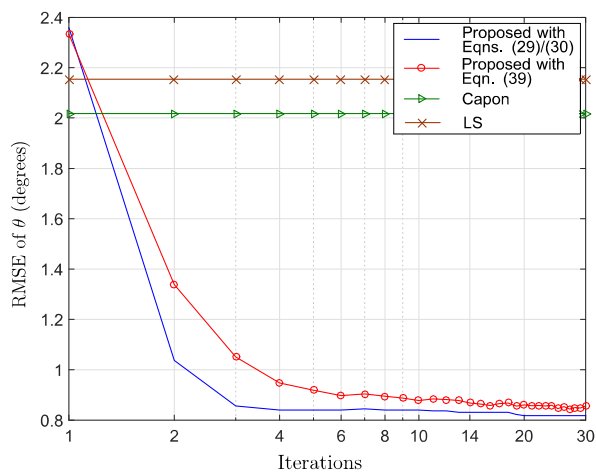


Fig. 11. The  $RMSE_{\theta}$  convergence of the proposed approach. The Tx and Rx arrays are ULAs with ( $N_{Tx} = 10, N_{Rx} = 15$ ) and half-wavelength interelement spacing.

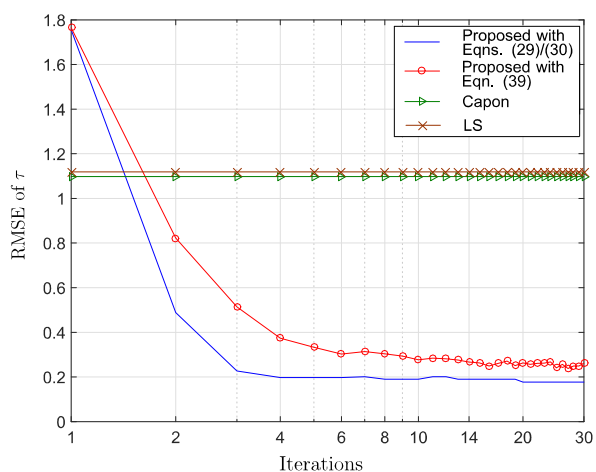


Fig. 12. The  $RMSE_{\tau}$  convergence of the proposed approach. The Tx and Rx arrays are ULAs with ( $N_{Tx} = 10, N_{Rx} = 15$ ) and half-wavelength interelement spacing.

or (39) significantly outperforms the traditional approaches such as LS and Capon due to the transmit beamforming gain brought by the proposed joint Tx–Rx optimization. Using 2000 computer simulation studies, the proposed approach with the (29)/(30) weights in the Step-6 has 100% successful convergence.

## VII. CONCLUSION

In this paper, a joint Tx–Rx multitarget localization approach has been proposed for MIMO radar systems that employ antenna arrays of known geometry. The proposed approach improves the performance of multitarget localization through the cooperation with Tx beamforming in an iterative way. In the proposed approach, the transmit beamforming design and the estimation of the target’s complex path gain are jointly derived from the same optimization problem that involves all the target parameters. Furthermore, the proposed DOA and Delay estimation method significantly enhances the resolution of the joint Tx–Rx multitarget localization approach.

## REFERENCES

- [1] E. Fishler, A. M. Haimovich, R. S. Blum, D. Chizhik, L. J. Cimini, and R. A. Valenzuela, “MIMO radar: An idea whose time has come,” in *Proc. IEEE Radar Conf.*, Apr. 2004, pp. 71–78.
- [2] A. M. Haimovich, R. S. Blum, and L. J. Cimini, “MIMO radar with widely separated antennas,” *IEEE Signal Process. Mag.*, vol. 25, no. 1, pp. 116–129, Jan. 2008.
- [3] J. Li and P. Stoica, “MIMO radar with colocated antennas,” *IEEE Signal Process. Mag.*, vol. 24, no. 5, pp. 106–114, Sep. 2007.
- [4] H. Commin, K. Luo, and A. Manikas, “Arrayed MIMO radar: Multi-target parameter estimation for beamforming,” in *Proc. Beamforming: Sensor Signal Process. Defence Applications*, 2015, pp. 119–158.
- [5] P. Stoica, J. Li, and Y. Xie, “On probing signal design for MIMO radar,” *IEEE Trans. Signal Process.*, vol. 55, no. 8, pp. 4151–4161, Aug. 2007.
- [6] D. R. Fuhrmann and G. S. S. Antonio, “Transmit beamforming for MIMO radar systems using signal cross-correlation,” *IEEE Trans. Aerosp. Electron. Syst.*, vol. 44, no. 1, pp. 171–186, Jan. 2008.
- [7] J. Li, P. Stoica, L. Xu, and W. Roberts, “On parameter identifiability of MIMO radar,” *IEEE Signal Process. Lett.*, vol. 14, no. 12, pp. 968–971, Dec. 2007.

- [8] L. Xu, J. Li, and P. Stoica, "Adaptive techniques for MIMO radar," in *Proc. 4th IEEE Workshop Sensor Array Multi-Channel Signal Process.*, Waltham, MA, USA, Jul. 2006, pp. 258–262.
- [9] L. Xu, J. Li, and P. Stoica, "Target detection and parameter estimation for MIMO radar systems," *IEEE Trans. Aerosp. Electron. Syst.*, vol. 44, no. 3, pp. 927–939, Jul. 2008.
- [10] J. Chen, G. Hong, and S. Weimin, "Angle estimation using ESPRIT without pairing in MIMO radar," *Electron. Lett.*, vol. 44, no. 24, pp. 1422–1423, 2008.
- [11] N. Liu, L.-R. Zhang, J. Zhang, and D. Shen, "Direction finding of MIMO radar through ESPRIT and Kalman filter," *Electron. Lett.*, vol. 45, no. 17, pp. 908–910, 2009.
- [12] W. Roberts, P. Stoica, J. Li, T. Yardibi, and F. A. Sadjadi, "Iterative adaptive approaches to MIMO radar imaging," *IEEE J. Sel. Topic Signal Process.*, vol. 4, no. 1, pp. 5–20, Feb. 2010.
- [13] M. Jin, G. Liao, and J. Li, "Target localisation for distributed multiple-input multiple-output radar and its performance analysis," *IET Radar, Sonar Navig.*, vol. 5, no. 1, pp. 83–91, Jan. 2011.
- [14] K. Luo and A. Manikas, "Superresolution multitarget parameter estimation in MIMO radar," *IEEE Trans. Geosci. Remote Sens.*, vol. 51, no. 6, pp. 3683–3693, Jun. 2013.
- [15] C. Chen, X. Zhang, and D. Ben, "Coherent angle estimation in bistatic multi-input multi-output radar using parallel profile with linear dependencies decomposition," *IET Radar, Sonar Navig.*, vol. 7, no. 8, pp. 867–874, Oct. 2013.
- [16] H. Li and B. Himed, "Transmit subaperturing for MIMO radars with co-located antennas," *IEEE J. Sel. Topic Signal Process.*, vol. 4, no. 1, pp. 55–65, Feb. 2010.
- [17] A. Hassaniien and S. Vorobyov, "Phased-MIMO radar: A tradeoff between phased-array and MIMO radars," *IEEE Trans. Signal Process.*, vol. 58, no. 6, pp. 3137–3151, Jun. 2010.
- [18] A. Manikas, *Beamforming: Sensor Signal Processing for Defence Applications*. London, U.K.: Imperial College Press, 2015.
- [19] W. M. Jang, B. Vojcic, and R. Pickholtz, "Joint Transmitter-Receiver optimization in synchronous multiuser communications over multipath channels," *IEEE Trans. Commun.*, vol. 46, no. 2, pp. 269–278, Feb. 1998.
- [20] D. Palomar, J. Cioffi, and M. Lagunas, "Joint Tx-Rx beamforming design for multicarrier MIMO channels: A unified framework for convex optimization," *IEEE Trans. Signal Process.*, vol. 51, no. 9, pp. 2381–2401, Sep. 2003.
- [21] T. Zhang and A. Manikas, "Joint transmitter-receiver beamforming over space-time fading channels," in *Proc. IEEE Int. Conf. Commun.*, Jun. 2007, pp. 4913–4918.
- [22] J. Hudson, *Adaptive Array Principles*. London, U.K. IEE, 1981.
- [23] M. Skolnik, *Radar Handbook*, 3rd ed. New York, NY, USA: McGraw-Hill, 2008.
- [24] M. Skolnik, *Introduction to Radar Systems*, 3rd ed. New York, NY, USA: McGraw-Hill, 2002.
- [25] H. Akaike, "A new look at the statistical model identification," *IEEE Trans. Autom. Control*, vol. 19, no. 6, pp. 716–723, Dec. 1974.
- [26] M. Wax and T. Kailath, "Detection of signals by information theoretic criteria," *IEEE Trans. Acoust. Speech, Signal Process.*, vol. ASSP-33, no. 2, pp. 387–392, Apr. 1985.
- [27] H.-T. Wu, J.-F. Yang, and F.-K. Chen, "Source number estimators using transformed Gerschgorin radii," *IEEE Trans. Signal Process.*, vol. 43, no. 6, pp. 1325–1333, Jun. 1995.
- [28] A. Manikas, *Differential Geometry in Array Processing*. London, U.K.: Imperial College Press, 2004.



**Kai Luo** (M'14) received the B.Eng. degree from the School of Electronics Information and Communications, Huazhong University of Science and Technology, Wuhan, China, in 2006, and the Ph.D. degree from the Department of Electrical and Electronic Engineering, Imperial College London, London, U.K., under the supervision of Prof. A. Manikas, in 2013.

In 2013, he joined the Institute of Electronics, Chinese Academy of Sciences, Beijing, China, and since 2014, he has been a Lecturer in the School of Electronics Information and Communications, Huazhong University of Science and Technology. His research interests include array signal processing, radar, MIMO communications and massive MIMO.



**Athanassios Manikas** (SM'02) holds the Chair of Communications and Array Signal Processing in the Department of Electrical and Electronic Engineering, Imperial College London, London, U.K. He has held a number of research consultancies for the EU, industry and government organisations. He has published an extensive set of journal and conference papers in the areas of wireless communications and array signal processing and is the author of a monograph entitled *Differential Geometry in Array Processing*. His main research interests include space-time wireless

communications, antenna arrays, array signal processing, beamforming, localization, uncertainties, mathematical modeling, analysis and algorithmic design, radar signal processing, MIMO radar, wireless sensor networks, 5G+, physical layer. He is leading a strong group of researchers at Imperial College and has supervised successfully more than 45 Ph.D.s and more than 200 Master's project-students.

He is a Fellow of the Institution of Engineering and Technology (IET), Fellow of the Institute of Mathematics and its Applications (IMA) and a Distinguished Lecturer of IEEE Communications Society. He is also the Chair of IEEE COMSOC TAOS Technical Committee. He is on various Editorial Boards and has had various technical chairs at international conferences, including the TPC Chair of IEEE ICC 2015 in London.